

**INTERNATIONAL JOURNAL OF ENGINEERING SCIENCES & RESEARCH  
TECHNOLOGY****NUMERICAL STUDY OF LONG COLUMNS STRENGTHENED BY FIBER  
REINFORCED POLYMER (FRP)****Ehab M. Lotfy, Acc. Prof.**

Civil Engineering Department, Faculty of Engineering, Suez Canal University, Egypt

DOI: 10.5281/zenodo.1246981

**ABSTRACT**

Strengthening of existing Reinforced Concrete structures is becoming a major issue in civil engineering. Externally Bonded Reinforcement (EBR) systems have been successfully applied for strengthening of existing concrete structures. This work includes a results of numerical models carried to investigate the behavior of reinforced concrete, RC, slender columns with rectangular sections under the effect of eccentric loads strengthened with carbon fiber-reinforced polymers (CFRPs) in three different manners in order to enhance its axial and flexural rigidity. The first approach is a well-known form of CFRP strengthening with sheet wrapping columns; the second approach is strengthening using CFRP sheets in longitudinal direction of columns, and a third one is a new retrofitting method of near surface mounted (NSM) CFRP strips. Ten full scale specimens with rectangular cross sections dimensions (210 × 150 mm) were tested under eccentric compressive loading to failure. The total length of all specimens was 3000 mm, with slender ratios 73, 60 and 50 respectively and characteristic strength 25, 35,45Mpa. NSM proved to be very effective in terms of increasing their flexural resistance, as long as the NSM bars can be effectively anchored in the adjacent long columns.

**KEYWORDS:** Strengthening, Long Columns, Fiber Reinforced Polymer**I. INTRODUCTION**

Worldwide application in reinforced concrete (RC) technology for the last 100 years have shown that RC structures exhibit a reliable and durable behavior when they are properly designed, built and maintained. However, porosity and cracking of concrete, as well as corrosion of steel reinforcement can lead to deficiency of existing RC structures especially when they are exposed to extreme and hostile environmental conditions and excessive loads. Other causes of structural deficiency are design mistakes, increase in load carrying needs, change of use of the structure, and adoption of more stringent design codes especially in seismic zones.

It is a well-known fact that the infrastructure of a country needs to be maintained either by demolishing the deficient structures and building new ones, or by rehabilitating the old ones with appropriate techniques to meet the current requirements for the continuity of modern civilization.

Unavoidably, countries which have had well established structural infrastructure for a long time are also the ones to have problems with it due to aging of existing structures. Australia's infrastructure condition was assessed to be in urgent need of rehabilitation especially for the highway bridges. However, no cost figure has been estimated for the rehabilitation. In USA, it was estimated that 40% of the 575000 highway bridges were either structurally deficient or obsolete, and 25% were over 50 years old and unsuitable for the current or projected traffic needs. The estimated cost for repairing all deteriorating bridges was US\$78 billion; however, only \$5 billion a year was available for such repairs. Over the years, engineers have used different methods and techniques to retrofit existing structures by providing external confining stresses. For the past few years, the concept of jacketing has been investigated to provide such forces. Externally applied jackets have been used as a reinforcement to contain concrete for different reasons. Engineers have used traditional materials such as wood, steel, and concrete to confine and improve the structural behavior of concrete members. Fiber reinforced composite materials are becoming more frequently used in civil engineering structures. One of the most practical applications of these new materials concerns the strengthening of reinforced concrete columns by means of confinement with fiber composite sheets. The typical confining techniques that are widely used for strengthening of columns, when it comes to columns with high slenderness ratio the confinement become more ineffective [1,2,3].



There are three methods to apply an FRP jacket to strengthen a column [4]: (1) in-situ wrapping of FRP sheets in a wet layup process; (2) in-situ formation of the jacket by filament winding; (3) use of prefabricated FRP shells. The most commonly used method is the in-situ wrapping method which is also used as a technique for strengthening in this present experimental study. The other two methods have been rarely used in practice. Study focuses on slender RC column strengthening. RC columns are generally referred to as vertical load carrying structural members. However, it is also known that this kind of classification is merely an idealization as columns may also carry shear and bending moments depending on their position in the structure, uneven settlements, workmanship errors and seismic loads. RC columns are constructed as highway bridge piers, vertical load carrying members in buildings or underground piles. They are constructed in many different cross sectional geometries and heights using different types and amounts of concrete and steel reinforcement depending on the structural necessity and material availability[1]. To keep RC columns from further deterioration due to materials' vulnerability to hostile environment conditions and to restore their strength, ductility and durability to a technically accepted level, there are a number of strengthening techniques developed and tested. Steel jacketing and Fiber Reinforced Polymer (FRP) wrapping are the most commonly used methods[5].

The most outstanding characteristic of the EBR technique is the ease and speed of installation compared to steel plate bonding. One of the drawbacks of EBR systems is the susceptibility to mechanical damages as well as to damage from environmental effects such as freeze thaw cycles due to direct exposure. Further, EBR systems are easily susceptible to damage by fire and vandalism. Although this technique is well established among the practitioners around the world, still there are some major concerns about some issues associated with this technique, for instance, premature debonding failures causing delamination of FRP reinforcement from the substrate at relatively low loads. The failure of a compression member has to do with the strength and stiffness of the material and the geometry (slenderness ratio) of the member. Whether a compression member is considered short, intermediate, or long depends on these factors [6]. Several design guidelines (fib 2001; ISIS 2001; ACI-440.2R 2002, 2008; JSCE 2002; CNR-DT200 2004; Concrete Society 2004) for external strengthening of RC structures using FRP composites have been published as a result of extensive research and enormous practical needs in this field. Nevertheless, relevant design provisions for FRP-confined RC columns in these design guidelines are only applicable to the design of short columns with negligible slenderness effects. Moreover, Only Concrete Society (2004) and ACI-440.2R (2008) have recommended a procedure to perform section analysis of short FRP-confined RC columns so that columns subjected to combined bending and axial compression can be designed accordingly, but they do not specify the corresponding design equations. Therefore, a proper design procedure for FRP-confined RC columns is urgently needed [7].

Various methods have been used to provide confinement to Short columns using FRP composites. Among them, in-situ FRP wrapping has been the most commonly used technique, in which fiber sheets or fabrics are impregnated with resins and wrapped continuously or discretely around columns in a wet lay-up process, with the main fibers solely or predominantly oriented in the hoop direction. This strengthening technique is potentially effective for columns of various section shapes, but is particularly effective for circular columns. Rectangular columns need to receive rounding of sharp corners or shape modifications before FRP jacketing to enhance the effectiveness of confinement. For example, a rectangular section may be modified into an elliptical section before FRP jacketing[8]. The Near Surface Mounted (NSM) FRP technique has emerged as a more effective strengthening technique than the EBR technique in many instances because of its ability to gain higher bond strengths and the possibility of precluding or delaying premature debonding failures, which are often observed in the EBR technique.

The NSM-FRP technique involves bonding FRP bars into precut grooves in the concrete cover of a structural member to be strengthened, using an adhesive as shown in Figures 1 & 2. The application of NSM technique covers both reinforced and pre stressed concrete structures as well as structures made of other materials, such as timber and masonry. Although only a limited number of research studies on NSM systems are currently available, the research carried out so far indicates that the NSM technique is a promising and effective technique in increasing both flexural and shear capacities of structural members such as beams [9, 10, 11, 12].

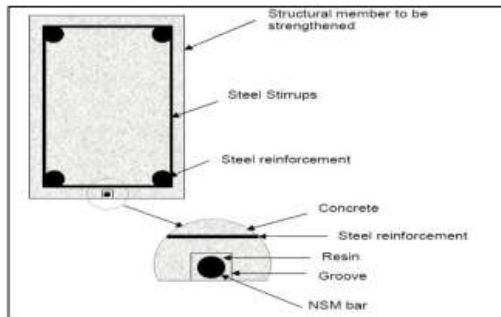


Figure 1. Arrangement of an NSM-FRP bar within the concrete cover

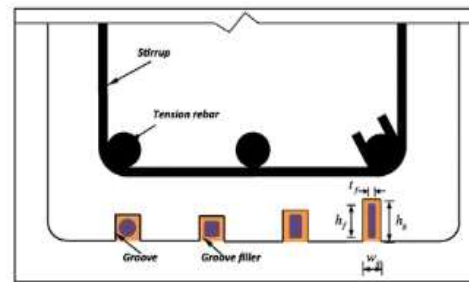


Figure 2. NSM-FRP bar shapes within the concrete cover

This work demonstrates different strengthening techniques to increase RC long columns capacity, with different slender ratios 73, 60 and 50 respectively, and characteristic strength 25, 35,45Mpa where the behavior is only controlled by buckling. The efficiency of different strengthening schemes is illustrated both experimentally and numerically. Based on test results, the most efficient technique is presented. It presents strengthening of long column with FRP where bending stresses due to buckling controls the design.

## II. OBJECTIVES

The main objective of the theoretical study can be summarized as follows:

1. Preparing a numerical model using (ANSYS 14.0) to simulate buckling, material non-linearity, to predict the failure mode, the crushing of concrete, and yielding of reinforced steel.
2. To produce a reasonable substitute of the test program to give more clear idea on the behavior of different types of retrofitting techniques using CFRP on slender columns.
3. To give a reasonable estimate for some data that was difficult to be measured experimentally like strain distribution on FRP sheets or NSM strips and the exact position failure.

## III. ΑΝΑΛΥΤΙΚΑ & ΝΥΜΕΡΙΚΑ ΣΤΥΔΨ

The numerical study has been decided to compare the experimental results for specimens. A proper finite element model has been used to idealize the considered structure in combination with experiments is necessary to formulate the material model and can greatly substitute an intensive experimental program [13].

The numerical modeling specimens were carried out using computer program based on nonlinear finite element technique (ANSYS 14.0) [14]. The details of strengthening column are shown in table 1.

The numerical modeling specimens were carried out using computer program based on nonlinear finite element technique; ANSYS 14.0. The details of strengthening column are shown in table 1. where all specimens have cross section 150\*210mm, 3000mm total length, main reinforcement 6#10mm and stirrups Ø6@100mm.

Table 1. :Details of tested specimens

Group	Specimens	$f_{cu}$ (N/mm <sup>2</sup> )	Slenderness ratio $\lambda$ ( $kl/r$ )	Strengthening schemes
G1	S1	25	73	Control
	S2			CFRP sheets (transverse direction)
	S3			CFRP sheets (Longitudinal direction)
	S4			CFRP sheets (Longitudinal direction+ transverse direction)
	S5			NSM-CFRP strips
	S6			NSM-CFRP strips + (transverse direction)
G2	S7	35	73	NSM-CFRP strips
	S8	45		NSM-CFRP strips
G3	S9	25	60	NSM-CFRP strips
	S10		50	NSM-CFRP strips

### A. Modeling of σπεχιμενοσ:

#### 1. Ελεμεντ Types

In the following subtitles the element types used to model concrete, steel case, machine head, interface (Bond), and material modeling is briefly described [15].

#### Χονχρετε

The concrete was modeled using 8 node solid element labeled by SOLID65 for the 3-D modeling of solids with or without reinforcing bars (rebar).

#### Steel Reinforcement

A Link180 element was used to model the steel reinforcement. Two nodes are required for this element [16].

#### ΦΡΠ

A layered solid element, Solid185, was used to model the FRP composites.

#### Steel Πλατεσ

An eight-node solid element, Solid 185, was used for the steel plates at the supports in the column models.

### 2. Ματεριαλ Properties

#### Χονχρετε

Concrete is a quasi-brittle material and has different behavior in compression and tension. The tensile strength of concrete is typically 8-15% of the compressive strength. Figure 3 shows a typical stress-strain curve for normal weight concrete.

#### Steel ρεινφορχεμεντ and steel plates

Steel reinforcement in the experimental columns was constructed with typical Grade 360 steel reinforcing bars. Properties, i.e., elastic modulus and yield stress, for the steel reinforcement used in this FEM study follow the design material properties used for the experimental investigation. The steel for the finite element models was assumed to be an elastic-perfectly plastic material and identical in tension and compression as shown in figure 4. Poisson's ratio of 0.3 was used for the steel reinforcement in this study shows the stress-strain relationship used in this study.

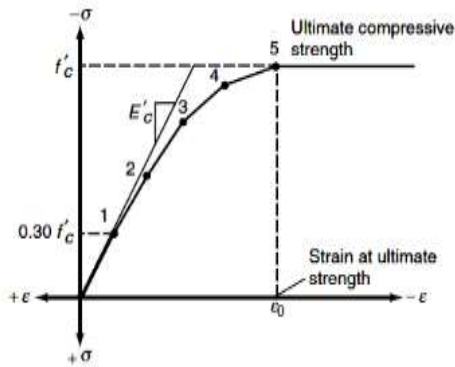


Figure 3: Typical uniaxial compressive and tensile stress-strain curve for concrete

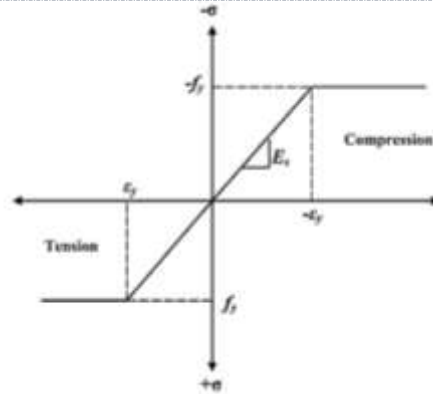


Figure 4: Stress-strain curve for steel reinforcement

**FRP ρεινφορχεμεντ modeling**

FRP material was modeled as linear-elastic up to failure as shown in figure 5 Different types of NSM-FRP reinforcement, (CFRP and GFRP) were used in this investigation. A full bond was assumed between the concrete and the FRP reinforcement.

**FRP Χομποσιτες**

FRP composites are materials that consist of two constituents. The constituents are combined at a macroscopic level and are not soluble in each other. One constituent is the reinforcement, which is embedded in the second constituent, a continuous polymer called the matrix. The reinforcing material is in the form of fibers, i.e., carbon and glass, which are typically stiffer and stronger than the matrix. The FRP composites are anisotropic materials; that is, their properties are not the same in all directions. Figure 6 shows a schematic of FRP composites.

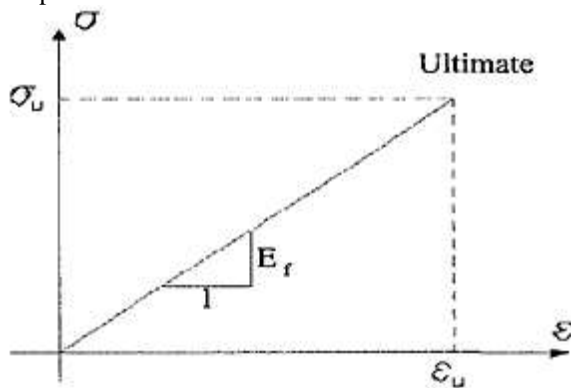


Figure 5: Stress-strain relationship for FRP

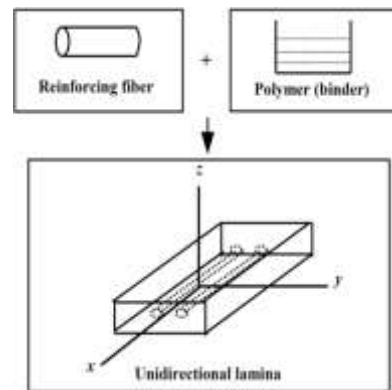


Figure 6: Schematic of FRP composites

**3. Γεομετρψ**

The dimensions of the Columns were 150 mm x 210 mm x 3000 mm. The two supports were at both ends of column (Hinged- Roller supports) as shown in figure 7. Figure 8 shows steel plate at column ends. Figure 9 shows typical steel reinforcement locations for the full-size columns. In the finite element models, 3-D spar elements, Link180, were employed to represent the steel reinforcement, referred to here as link elements; Figure 10 shows typical FRP NSM reinforcement locations for the full-size columns. In the finite element models, 3-D spar elements, Link180, were employed to represent the NSM reinforcement, referred to here as link elements. Figure 11 shows the bond strength between the concrete and steel reinforcement should be considered. However, in this study, perfect bond between materials was assumed. To provide the perfect bond, the link element for the steel reinforcing was connected between nodes of each adjacent concrete solid element, so the two materials shared the same nodes.

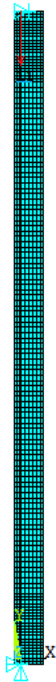


Figure 7: The two supports were at both ends of column (Hinged-Roller supports)



Figure 8: steel plate at column ends.



Figure 9: shows typical steel reinforcement locations

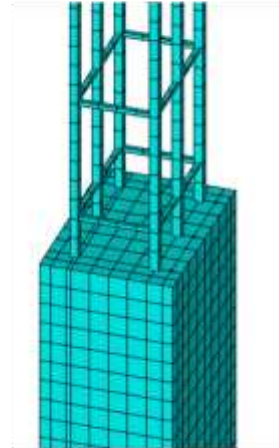


Figure 10: typical FRP NSM reinforcement locations

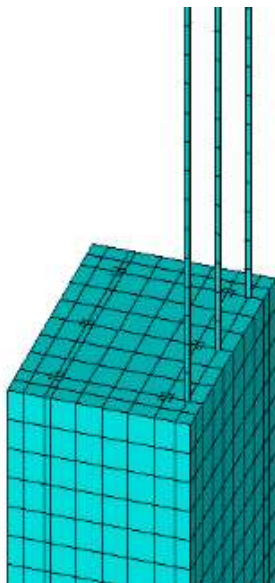


Figure 11: typical FRP longitudinal Sheet locations



**B. Λοαδινγ and Boundary Conditions**

All columns were tested in uniform loading at the free ends, the finite element models were loaded at the same locations with the same method. In the experiment, the uniform load applied over the column head plate. In FEM the load applied as pressure on this area. A 30 thick steel plate, modeled using Solid185 elements, was added at the two ends locations (loading and support locations) in order to avoid stress

concentration problems. This provided a more even stress distribution over the support area. Moreover, two supports were placed under the eccentricity  $e_0$  of the steel plate to allow rotation of the plate.

The ANSYS program uses Newton-Raphson equilibrium iterations for updating the model stiffness. For the nonlinear analysis, automatic stepping in ANSYS program predicts and controls load step size. The maximum and minimum load step sizes are required for the automatic time stepping.

### Ι. ΦΙΝΙΤΕ ΕΛΕΜΕΝΤ ΠΕΣΥΛΤΣ ΑΝΔ ΔΙΣΧΥΣΣΙΟΝ

The parametric investigate the behavior of reinforced concrete, RC, slender columns with rectangular sections under the effect of eccentric loads strengthened with carbon fiber-reinforced polymers (CFRPs) in three different manners in order to enhance its axial and flexural rigidity. The first approach is using CFRP strengthening with sheet wrapping columns; the second approach is strengthening using CFRP sheets in longitudinal direction of columns, and a third one is a new retrofitting method of near surface mounted (NSM) CFRP strips, with different slender ratios 73, 60 and 50 respectively, and characteristic strength 25, 35, 45 Mpa. Table 2 shows the numerical results of tested specimens

**Table 2:** Numerical results of tested specimens

Group	Spec.	$f_{cu}$ (N/mm <sup>2</sup> )	Slenderness ratio ( $\lambda=KL/r$ )	Pu (Kn)	Def. (mm)	T (Kn.mm)	Strengthening schemes
G1	S1	25	73	315	19	4020	Control
	S2			328	21	4473	CFRP sheets (tran. direction)
	S3			350	15	3664	CFRP sheets (Long. direction)
	S4			360	20	5410	CFRP sheets (Long. direction+ tran. direction)
	S5			355	17	3715	NSM-CFRP strips
	S6			365	25	6720	NSM-CFRP strips + (tran. direction)
G2	S7	35	73	400	20	5262	NSM-CFRP strips
	S8	45		420	23	6972	NSM-CFRP strips
G3	S9	25	60	380	22	5840	NSM-CFRP strips
	S10		50	400	24	7282	NSM-CFRP strips

Long.: Longitudinal      tran.: transverse      T: Toughness      Spec. :Specimens

The following subtitles compare the results of the numerical results with the experimental data for the test columns[17]. The following comparisons are made: load-strain plots at selected locations; load-deflection plots at mid height; loads at failure; and crack patterns of the internal concrete core at failure. Also discussed are the summaries of the maximum stresses occurring in outer steel case for the finite element models.

#### 1. Validation of the Proposed Finite Element Model

In the following section, a validation for the proposed model is made by a comparison between the experimental and the numerical results for test specimens S1to S6. The output responses of interest are the load deflection profile, ultimate load carrying capacity and debonding strain in NSM-FRP bars. The comparison shows good agreement between the numerical and experimental results as shown in figure 12.

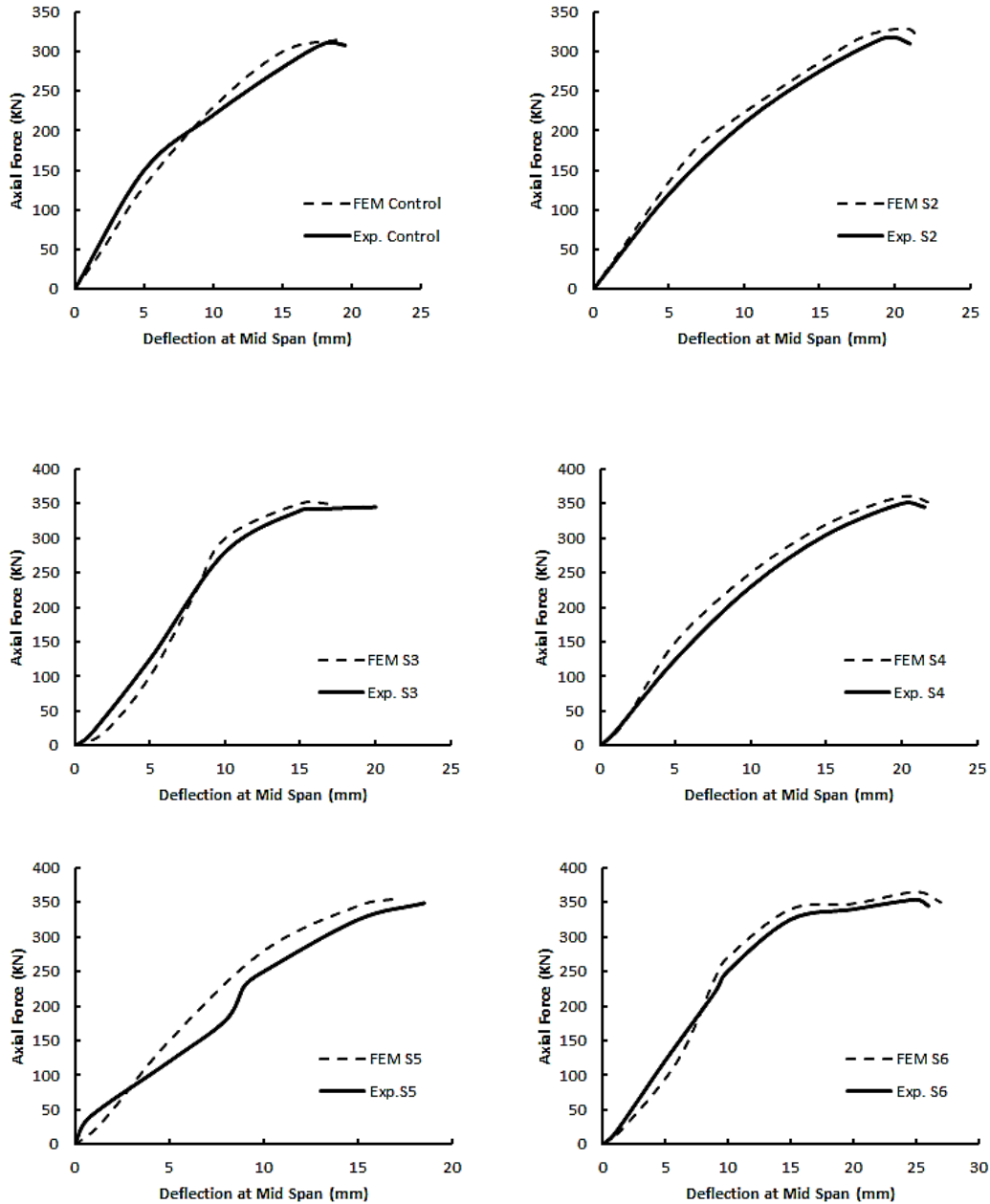
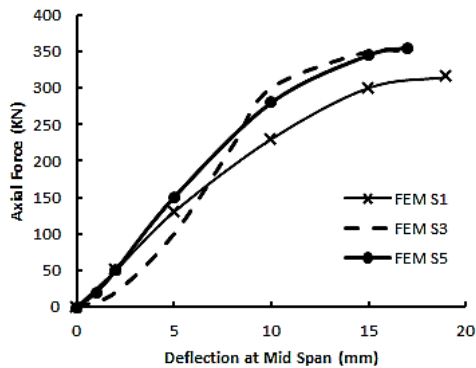


Figure 12: The numerical and experimental load-deformation curve of tested columns

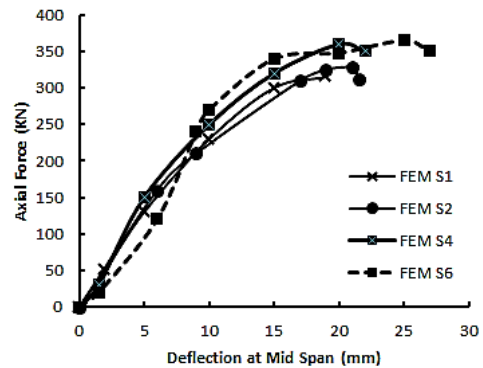
**2. The Effect of Strengthening Technique**

Figures 13 shows the numerical load-deformation of columns S1, S3, and S5, which have different strengthening technique; control specimen, CFRP sheets (Longitudinal direction), and NSM-CFRP strips. Where Figures 14 shows the numerical load-deformation of columns S1, S2, S4 and S6, which have different strengthening technique; control specimen, CFRP sheets (transverse direction), CFRP sheets (Longitudinal direction and transverse direction), and (NSM-CFRP strips and transverse direction) respectively





Figures 13: Numerical load-deformation of columns S1, S3, and S5



Figures 14: Numerical load-deformation of columns S1, S3, and S5

From Table 2, it can be seen that, ultimate loads and maximum deflection of S2, S3, S4, S5 and S6 to S1 are (104,111, 114, 113 and 116%) and (111, 79, 105, 89 and 132%) respectively as shown in figures 15, 16.

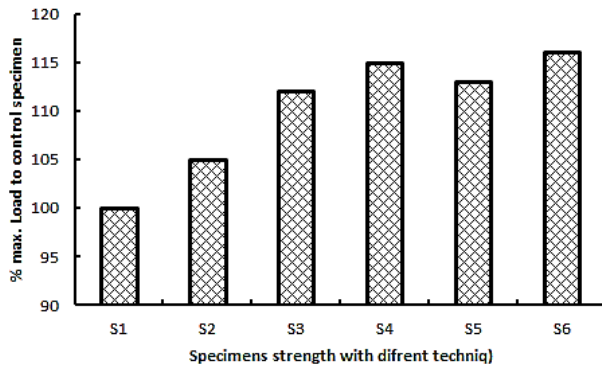


Figure 15: Different strengthening technique and ultimate load of control specimens

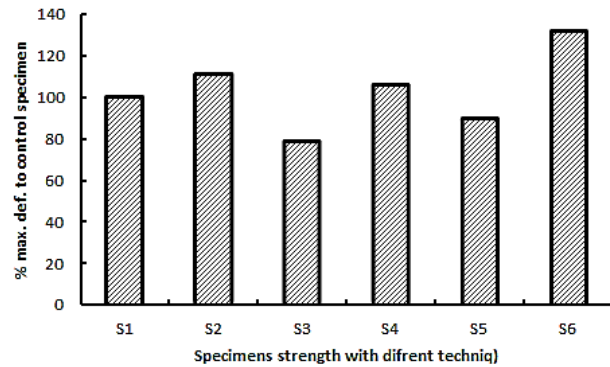


Figure 16: Different strengthening technique and maximum deflection of control specimens

Using CFRP sheets (Longitudinal direction), and NSM-CFRP strips increase the ultimate loads of specimens by 111 and 113% of control specimens, where using CFRP sheets (transverse direction) with Longitudinal direction and NSM-CFRP strips increase the maximum deflection by 105 and 132%

Using longitudinal NSM-CFRP strips tend to be more effective to prevent eventual debonding of CFRP strips in compression and to ensure the stability of the epoxy adhesive

The most efficient strengthening method for improving flexural capacity has been demonstrated experimentally by a combination of the NSM-CFRP reinforcement and the CFRP wrapping.

### 3. The Effect of Slenderness Ratios

Figure 17 shows the numerical load-deformation of columns S5, S7, and S8, which have characteristic strength 25, 35, 45 MPa respectively with NSM-CFRP strips.

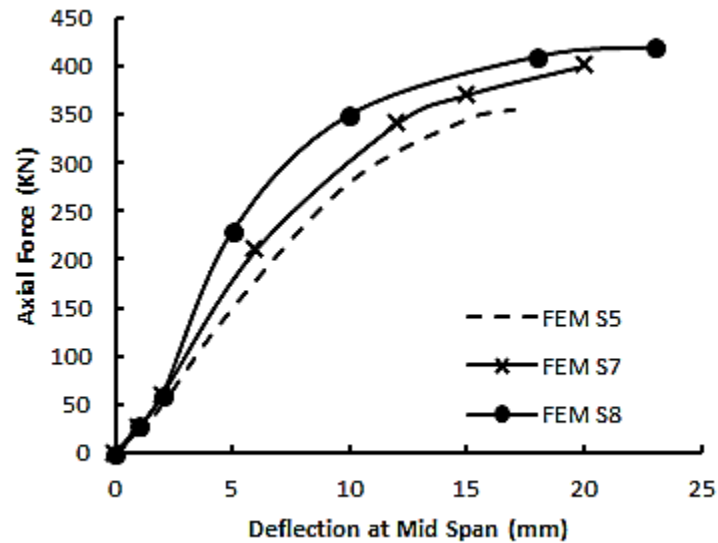


Figure 17: Numerical load-deformation of columns S5, S7, and S8

From Table 2, it can be seen that, ultimate loads, maximum deflection and toughness of S7 and S8 and S5 are (113 and 118%), (118 and 135%) and (181 and 142%) respectively.

Using NSM-CFRP strips in strengthened specimens with characteristic strength ( $f_{cu} = 45$  MPa) has a significant effect in the behavior of specimens more than specimens with characteristic strength ( $f_{cu} = 25$  and 35 MPa).

#### 4. The Effect of Slenderness Ratios

Figure 18 shows the numerical load-deformation of columns S5, S9, and S10, which have slenderness ratios 73, 60 and 50 respectively with NSM-CFRP strips.

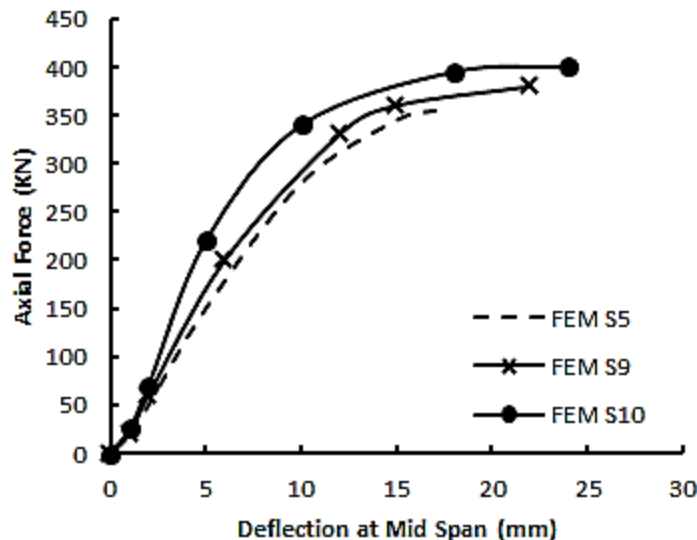


Figure 18: Numerical load-deformation of columns S5, S9, and S10

From Table 2, it can be seen that, ultimate loads, maximum deflection and toughness of S9 and S10 and S5 are (107 and 113%), (129 and 141%) and (157 and 196%) respectively.

Using NSM-CFRP strips in strengthened specimens with slenderness ratio ( $\lambda = 50$ ) has a significant effect in the behavior of specimens more than specimens with slenderness ratios ( $\lambda = 60$  and 73).

ζ. ΑΝΑΛΥΤΙΚΑ ΣΤΥΔΨ

Numerical analysis was carried out before column testing with measured material properties according to a number of analytical models found from various sources, which were then modified following the results of the experimental investigation. The models, which primarily corresponded with experimental results, are further recommended for typical use. In the preliminary part of the analytical procedure, interaction diagrams (IDs) were developed for slender columns as the most convenient method for discussing the effects of variables on column resistance. The load-maximum moment curves (at the mid-height for columns with hinged supports at both ends), for a given slenderness  $\lambda$  and initial end eccentricity  $e_{01}$ , is shown by line 0-B<sub>1</sub>. The column fails when this line intersects the ID, at point B<sub>1</sub>. At this point, the load and moment at the column ends are given by point A<sub>1</sub>. The same relationship holds for line 0-B<sub>2</sub> at end eccentricity  $e_{02}$ . This indicates that the interaction diagram for a slender column with a given slenderness  $\lambda$  can be obtained by repeating this process a number of times with different end eccentricities  $e_{0j}$ . The maximum load capacity  $N_R$  can be determined from the linear relationship between the compression force  $N$  and the first order bending moment  $M_0$ . Compression force  $N_R$  and total bending moment  $M_R$  act in the most stressed cross section. This moment is the sum of bending moments of first ( $M_{R,0}$ ) and second orders ( $M_{R,II}$ ) as shown in figure 19.

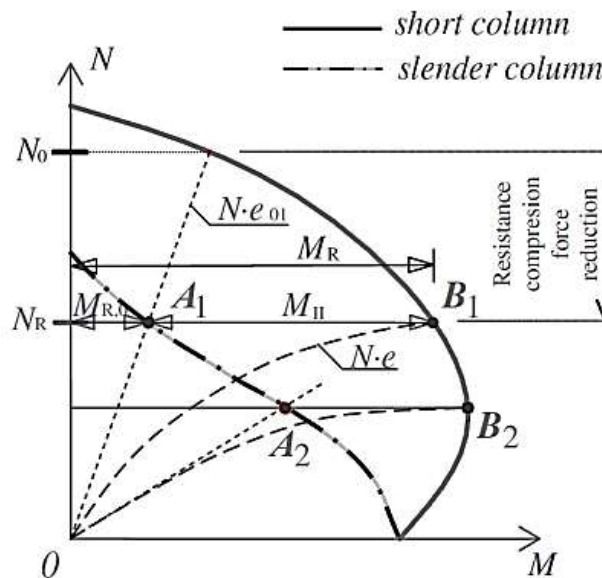


Figure 19: Interaction diagrams for short and slender columns

$$M_R = M_{R,0} + M_{R,II} \dots\dots\dots(N.m) \tag{1}$$

The resistance of reinforced concrete cross section, defined by  $N_R$ – $M_R$ , is calculated as follows from the equilibrium equations:

$$N_R = F_{cc} + \Sigma F_{si} \dots\dots\dots(N) \tag{2}$$

$$M_R = F_{cc} * Z_c + \Sigma (F_{si} * Z_{si}) \dots\dots\dots(N.m) \tag{3}$$

Where  $F_{cc}$  = compression force in concrete;  $z_c$  = distance of compression force in concrete from gravity center axis of concrete cross section;  $F_{si}$  = force in steel reinforcement in row i; and  $z_{si}$ =distance of force in row i of steel reinforcement from gravity center axis of concrete cross section.

The interaction diagrams are calculated by assuming a series of strain distributions. Stresses for force calculations are then determined from stress-strain relationships of each material and Eqs. (2) and (3) are quantified. In each point of the section interaction diagram, the real reduced bending stiffness  $(EI)_r$  can be calculated and used for determination of curvature, including second-order effects. Following this curvature, a first-order bending moment can be derived to present a slender column interaction diagram.

The second part of the analytical procedure involves the inclusion of the strengthening effects to the column resistance. NSM-CFRP strips in the grooves are considered as additional reinforcement near the cross-section surface and the values of their strains are determined based upon concrete strains, depending on their distance from the neutral axis Figure 20. From the strain values of the CFRP strips, the stress is determined from a linear

stress-strain relationship. The same stress-strain diagram is used both in tension and compression. It is very important to make provision for initial strains in the reinforced concrete section when the CFRP strips are applied. During strengthening the structure is maximally relieved, even though there are some low strains in the concrete and steel reinforcement, and it is necessary for them to be included. The theoretical initial strain values of CFRP strips after unloading ( $\epsilon_{f,un}$ ) are subtracted. Equilibrium equations are then adjusted as follows:

$$N_R = F_{cc} + \Sigma F_{si} + \Sigma F_{fi} \dots\dots\dots(N) \quad (4)$$

$$M_R = F_{cc} * Z_c + \Sigma (F_{si} * Z_{si}) + \Sigma (F_{fi} + Z_{fi}) \dots\dots\dots(N.m) \quad (5)$$

Where:  $F_{fi}$  = force in CFRP strips in row  $i$ , and  $z_{fi}$  = distance of force in row  $i$  of CFRP strips from gravity center axis of concrete cross section

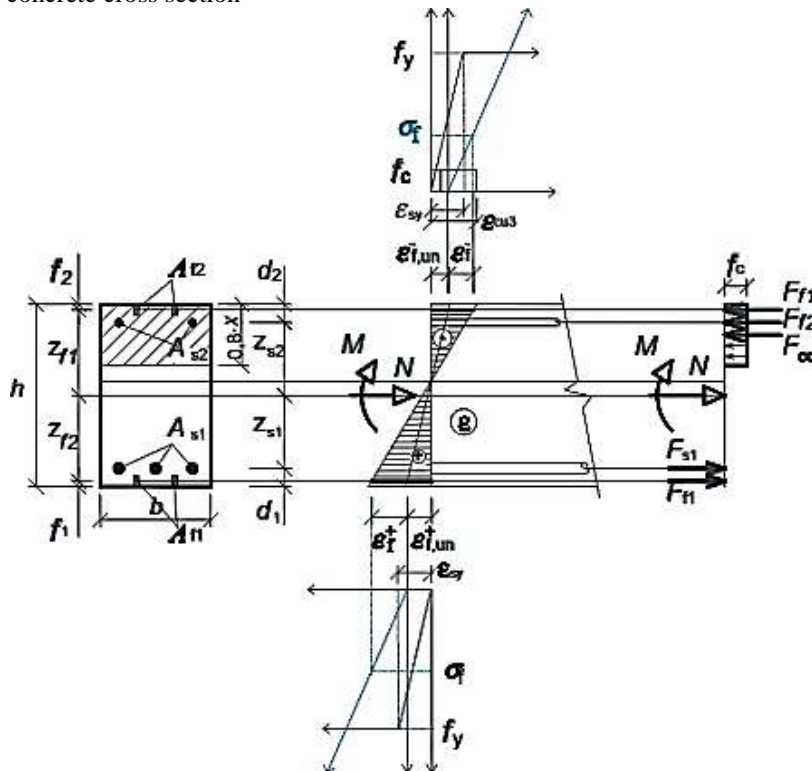


Figure 20: Forces in cross section strengthened with longitudinal CFRP strips

**Σimplified analysis of singly reinforced rectangular sections**

**Failure modes**

The possible failure modes of beams flexural-strengthened with NSM CFRP reinforcement are of two types: those of conventional RC beams, including concrete crushing or NSM-CFRP rupture generally after the yielding of internal steel bars, for which the composite action between the original beam and the NSM CFRP is practically maintained up to failure, and “premature” debonding failure modes which involve the loss of this composite action. Although debonding failures are less likely a problem with NSM-CFRP compared with externally bonded FRP, they may still significantly limit the efficiency of this technology. In the present analysis, it is assumed that the beam is properly detailed so as to preclude debonding failure modes.

**Assumptions of present analysis**

The design equations presented herein are based on the following assumptions:

- Linear strain distribution across the section depth.
- Compressive force in concrete, at crushing, is determined by Whitney’s equivalent rectangular stress block. The ultimate compressive strain in concrete is assumed to be 0.0035.
- Tensile stresses in concrete, at ultimate strength, are ignored.
- Reinforcing steel is assumed to have elastic-perfectly plastic response.
- CFRP behaves linearly up to brittle failure since its fibers are aligned with the beam axis.
- Perfect NSM-CFRP strip bond is considered for strain compatibility equations.

- The governing failure mode is concrete crushing, preceded by steel yielding, prior to CFRP rupture. A minimum NSM-CFRP ratio is formulated to ensure this failure mode.

The approach developed is followed here, as closed form equations are formulated to establish a direct procedure for flexural strength design of FRP strengthened beams. They differ from the current state of the art iterative procedure which may lead to tedious calculations. Referring to Figure 21, the force equilibrium equation is used to define the CFRP strip ratio as follows:

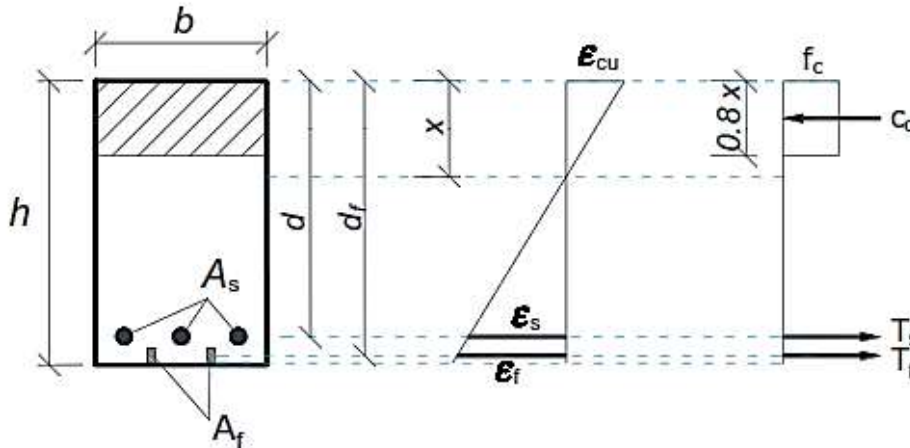


Figure 21: singly reinforced cross-section with strain distribution and force profile.

$$A_f = \frac{f_c ab - A_s f_y}{f_f} \quad (6)$$

With  $f_c = 0.8 f_{cu}$  and  $a = 0.8x$

$$\rho_f = \frac{f_c}{f_f} 0.8 \alpha - \frac{f_s}{f_f} \quad (7)$$

Where  $\rho_f = \frac{A_f}{bd}$ ,  $\rho_s = \frac{A_s}{bd}$ ,  $\alpha = \frac{x}{d}$

Using strain compatibility, the strain in the NSM-CFRP strip is given by:

$$\epsilon_f = \frac{d_f - x}{x} \epsilon_{cu} \quad (8)$$

Considering that  $\alpha_d = \frac{d_f}{d}$ , the above equation is rewritten as follows

$$\epsilon_f = \left( \frac{\alpha_f}{\alpha} - 1 \right) \epsilon_{cu} \quad (9)$$

Where:  $\epsilon_f$  is the CFRP strain at failure.

Thus, the tensile stress in NSM-CFRP strip is

$$f_f = \epsilon_f E_f = \left( \frac{\alpha_f}{\alpha} - 1 \right) \epsilon_{cu} E_f \quad (10)$$

The expression of the ultimate moment of resistance may be obtained by summing the moment of the forces acting on cross section about the centroid of the concrete stress block

$$M_r = A_s f_y (d - 0.4x) + A_f f_f (d_f - 0.4x) \quad (11)$$

## 5.1. CONCLUSION

The Nonlinear behavior of 10- long columns are investigated in the current study under the effect of increasing loading employing the inelastic FEM analysis by program ANSYS. Several parameters are investigated including three different manners to enhance axial and flexural rigidity. The first approach is using CFRP strengthening with sheet wrapping columns; the second approach is strengthening using CFRP sheets in longitudinal direction of columns, and a third one is a new retrofitting method of near surface mounted (NSM) CFRP strips, with different slender ratios 73, 60 and 50 respectively, and characteristic strength 25, 35, 45 Mpa. The study focuses on the consequences of the investigated parameters on the deformation and ultimate resisting load. The conclusions made from this investigation are:

- Using longitudinal direction CFRP sheets and NSM-CFRP strips increase the ultimate loads of specimens by 111 and 113% of control specimens.
- Using transverse direction CFRP sheets with longitudinal direction and NSM-CFRP strips increase the maximum deflection by 105 and 132%
- Using longitudinal NSM-CFRP strips tend to be more effective to prevent eventual debonding of CFRP strips in compression and to ensure the stability of the epoxy adhesive
- The NSM-CFRP strips embedded longitudinally works effectively in tension which takes place at the minor bending axis of the slender columns where the second order (buckling) effect takes place results in an increase in the bending moment at the same compression force value.
- The most efficient strengthening method for improving flexural capacity has been demonstrated experimentally by a combination of the NSM-CFRP reinforcement and the CFRP wrapping.
- Using NSM-CFRP strips in strengthen specimens with characteristic strength ( $f_{cu}= 45$  MPa) has a significant effect in the behavior of specimens more than specimens with characteristic strength ( $f_{cu}= 25$  and 35 MPa).
- Using NSM-CFRP strips in strengthen specimens with slenderness ratio ( $\lambda=50$ ) has a significant effect in the behavior of specimens more than specimens with slenderness ratios ( $\lambda =60$  and 73).
- Simplified analysis of singly reinforced rectangular sections with NSM-CFRP strips:  
The expression of the ultimate moment of resistance may be obtained by summing the moment of the forces acting on cross section about the centroid of the concrete stress block

$$M_r = A_s f_y (d - 0.4X) + A_f f_f (d_f - 0.4X)$$

$$f_f = \varepsilon_f E_f = \left( \frac{\alpha_f}{\alpha} - 1 \right) \varepsilon_{cu} E_f$$

$$\varepsilon_f = \left( \frac{\alpha_f}{\alpha} - 1 \right) \varepsilon_{cu}$$

$$\varepsilon_f = \frac{d_f - X}{X} \varepsilon_{cu}$$

Where:  $\varepsilon_f$  is the CFRP strain at failure.

## REFERENCES

- [1] Yazici, V., "Strengthening hollow reinforced concrete columns with fibre reinforced polymers" Doctor of Philosophy thesis, School of Civil, Mining and Environmental Engineering, University of Wollongong, 2012.
- [2] McShane, I., "Social value and the management of community infrastructure" Australian Journal of Public Administration, 2006. **65**(4): p. 82-96.
- [3] Marshall Jr, O., R. Lampo, and J. Busel. "IN-PLACE STRENGTHENING, REPAIR OR UPGRADE OF CONCRETE CIVIL ENGINEERING STRUCTURES USING FIBER REINFORCED POLYMERIC COMPOSITE MATERIALS" First International Conference on Composites in Infrastructure. 1996.
- [4] Lam, L. and J. Teng, "Design-oriented stress-strain model for FRP-confined concrete in rectangular columns". Journal of Reinforced Plastics and Composites, 2003. **22**(13): p. 1149-1186.
- [5] Priestley, M.N., F. Seible, and G.M. Calvi, "Seismic design and retrofit of bridges" John Wiley & Sons, New York, 686 p, 1996.
- [6] Mirmiran A., M. Shahawy, and T. Beitleman, *Slenderness limit for hybrid FRP- concrete columns*. Journal of Composites for Construction, 2001. **5**(1): p. 26-34.
- [7] Jiang, T., "FRP-confined RC columns: analysis, behavior and design" Ph.D. thesis, The Hong Kong Polytechnic University, Hong Kong, China The Hong Kong Polytechnic University, 2008.
- [8] Teng JG, Chen JF, Smith ST, Lam L (2002) FRP: strengthened RC structures. *Frontiers in Physics*, p: 266.
- [9] Hassan T. and S. Rizkalla, "Investigation of bond in concrete structures strengthened with near surface mounted carbon fiber reinforced polymer strips". Journal of composites for construction, 2003. **7**(3): p. 248-257.
- [10] De Lorenzis, L., B. Miller, and A. Nanni, "Bond of FRP laminates to concrete". ACI Materials Journal, 2001. **98**(3): p. 256-264.



- 
- [11] Micelli, F. and A. Nanni, "Durability of FRP rods for concrete structures" Construction and Building materials, 2004. **18**(7): p. 491-503.
  - [12] Hassan, T. and S. Rizkalla, "Bond mechanism of NSM FRP bars for flexural strengthening of concrete structures". ACI Structural Journal, 2004. **101**(6): p. 830-839.
  - [13] Aad, G., "The ATLAS simulation infrastructure". The European Physical Journal C, 2010. **70**(3): p. 823-874.
  - [14] Hawileh, R.A., "Nonlinear finite element modeling of RC beams strengthened with NSM FRP rods". Construction and Building Materials, 2012. **27**(1): p. 461-471.
  - [15] Shahawy, M., A. Mirmiran, and T. Beitelman, "Tests and modeling of carbon-wrapped concrete columns". Composites Part B: Engineering, 2000. **31**(6): p. 471-480.
  - [16] Barbero, E.J., Finite element analysis of composite materials using Abaqus<sup>TM</sup>. 2013: CRC press.
  - [17] Selmy YASSER, Lotfy EHAB, El-Kersh IBRAHIM "BEHAVIOR OF LONG COLUMNS STRENGTHENED BY CFRP SHEETS AND NEAR SURFACE MOUNTED STRIPS" INTERNATIONAL CONFERENCE ON ADVANCED CIVIL ENGINEERING AND TRANSPORTATION, ACET, April 15-16,2018, SHANGHAI, CHINA.